Received: 16 July 2019 | Revised: 24 August 2019 | Accepted: 25 August 2019

DOI: 10.1002/jrs.5741

RESEARCH ARTICLE

WILEY Journal of RAMAN SPECTROSCOPY

Detection and identification of canker and blight on orange trees using a hand-held Raman spectrometer

Lee Sanchez[1] | **Shankar Pant**[2] | **Mike Irey**[3] | **Kranthi Mandadi**[2,4] | **Dmitry Kurouski**[1,5]

[1]Department of Biochemistry and Biophysics, Texas A&M University, College Station, Texas 77843

[2]Texas A&M AgriLife Research and Extension Center, Weslaco, Texas 78596

[3]Southern Gardens Citrus, Clewiston, Florida 33440

[4]Department of Plant Pathology, Texas A&M University, College Station, Texas 77843

[5]The Institute for Quantum Science and Engineering, Texas A&M University, College Station, Texas 77843

Correspondence
Dmitry Kurouski, Department of Biochemistry and Biophysics, Texas A&M University, College Station, Texas 77843.
Email: dkurouski@tamu.edu

Funding information
Governor' University Research Initiative (GURI), Grant/Award Number: 12-2016/M1700437; Texas A&M AgriLife Research Insect Vectored Diseases Seed Grant, Grant/Award Number: 124185-96210; Governor's University Research Initiative (GURI), Grant/Award Number: 12-2016/M1700437; T3 grant

Abstract

Huanglongbing (HLB), or citrus greening, is a devastating disease of citrus that is debilitating the U.S. citrus industry. The infected trees exhibit yellowing leaves, premature defoliation, and ultimately death of the entire plant. In addition to the devastating impact of HLB alone, infected trees become an easy target for other diseases. This further decreases the fruit yield, shortens the tree life, and complicates management practices. Raman spectroscopy is a noninvasive and nondestructive analytical technique that provides insight on the chemical structure of a specimen. In this study, we demonstrate that utilization of a hand-held Raman spectrometer in combination with chemometric analyses enables detection and identification of the secondary disease such as blight on HLB-infected orange trees (HLB + BL). We also showed that using this spectroscopic approach, we could detect and identify canker and distinguish this disease from healthy trees, HLB, and HLB + BL with high accuracy.

KEYWORDS

blight, canker, HLB, plant diseases, Raman spectroscopy

1 | INTRODUCTION

Huanglongbing (HLB) or citrus greening is a sad reality for nearly all citrus producers in Florida. The infected trees exhibit yellowing leaves, premature defoliation, and ultimately death of the entire plant. This all causes a significant reduction in the fruit yield and preliminary drop of the fruits. Not only does this disease plague citrus trees in the United States but also in Asia and Africa.[1] It is associated with *Candidatus* Liberibacter spp., a gram-negative bacterium that inhabits the plant phloem in uneven and variable titers.[2,3] The bacteria are psyllid-transmitted, which enables rapid proliferation of HLB on large agricultural areas. Unsurprisingly, HLB has spread to Texas, another major citrus producing state in the country, and has more recently made its way to California. Although direct removal of infected trees would be the most effective approach to prevent further spread the disease, this would decrease yield in the short term as those trees still produce marketable fruits.

HLB-infected citrus trees become an easy target for secondary diseases such as blight. Appearance of blight on citrus trees further decreases their fruit yield and shortens the tree life. Citrus blight is one of the

devastating diseases of citrus, mainly in hot and humid citrus producing areas, and was first described over 100 years ago.[4] Despite the several efforts, there is no clear understanding about the cause of blight and its pathology. The characteristic symptoms of blight include zinc deficiency in leaves and die back of twig.[5–7] One of the bottlenecks in studying blight disease is lack of reliable, quick, and sensitive disease diagnostic method. The current methods used to detect blight disease include water uptake test,[8] examination of zinc and water-soluble phenolic levels in the wood,[9] and serological assays for a protein associated with citrus blight (p12).[10]

Citrus canker, caused by a bacterium, *Xanthomonas axonopodis* pv. *citri*[11] (synonym: *X. campestris* pv. *citri*), is another devastating disease of citrus in many tropical and subtropical citrus-producing areas worldwide.[12,13] Appearance of canker disease triggers an immediate quarantine of the outbreak areas, as well as eradication measures, ceasing the movement/trade of fresh fruits, causing enormous economic loss.[13,14] Citrus canker is characterized by the formation of crater-like lesions in leaves, defoliation, fruit drops, and dieback.[15,16] Detection and identification of canker disease in early stages of infection is necessary for effective disease management and a better understanding of disease development. The commonly used techniques for detection and identification of canker in citrus are DNA-based assays such as polymerase chain reaction (PCR), and quantitative real-time PCR (qPCR),[17,18] and serological tests (enzyme-linked immunosorbent assay).[12,19] However, these techniques come with certain limitations such as low sensitivity, invasive/destructive to sample specimen, portability of machine, labor intensive, costly, and need specific expertise. These limitations catalyzed a search for a minimally invasive, fast, and confirmatory method that would enable highly accurate detection and identification of canker and blight disease on HLB-infected plants.

Raman spectroscopy (RS) is a label-free, noninvasive, nondestructive rapid and portable spectroscopic technique that can be used to determine structure and composition of analyzed specimens. We have recently demonstrated that using a hand-held Raman spectrometer, we could detect and identify fungal diseases in maize.[20] We also showed that RS was capable of diagnosis of ergot, black tip, and mold on wheat and sorghum.[21] Additionally, we showed that RS could detect insects inside intact cowpeas with high statistical accuracy.[22] Finally, we demonstrated that RS could be used to distinguish between healthy, HLB (early and late stage)-infected citrus trees, and suffering from nutrient deficits.[23] The detection rates of Raman-based diagnostics of healthy versus HLB infected versus nutritional were ~98% for grapefruit and ~87% for orange trees, whereas the accuracy of early versus late stage HLB infected was ~85% for grapefruits and ~94% for oranges. Leveraging this technology, we wanted to investigate whether RS can be used to detect and identify secondary diseases such as blight on HLB-infected trees, as well as diagnose canker on orange trees and distinct both canker and blight from HLB and healthy trees.

2 | MATERIALS AND METHODS

2.1 | Plants

Orange (*Citrus sinensis*, Valencia) field samples were collected from the orchards of Southern Garden Citrus (FL). Twelve to 21 leaves were randomly collected from each healthy (HL), HLB early (asymptomatic) (HLB), HLB trees with blight (HLB-BL), and trees with symptoms of canker (CA). Leaf samples were carefully selected to be devoid of physical or insect damage as well as symptoms unrelated to HLB, BL, and CA. Samples were kept in Ziploc bag and immediately brought to lab for RS and qPCR analysis.

2.2 | Raman spectroscopy

Following collection of the citrus leaves in-field, Raman spectra were taken with a hand-held Resolve Agilent spectrometer equipped with 831-nm laser source. The following experimental parameters were used for all collected spectra: 1-s acquisition time, 495-mW power, and baseline spectral subtraction by device software. Four spectra were collected from each leaf from four quadrants on the adaxial side of the leaf. In total, around 50 surface spectra from each group (HL, HLB, CA, and HLB-BL) were collected. Spectra shown in the manuscript are raw baseline corrected, without smoothing.

2.3 | DNA extraction

After taking Raman spectra readings, DNA was extracted from the midrib of each leaf using Biopsprint 96 DNA Plant Kit on a Qiagen Biosprint robot according to the manufacturer's protocol. Briefly ~100 mg of finely sliced leaf tissue was homogenized in 2-ml microcentrifuge tubes for 45 s in a Biospec Mini-Beadbeater 96 (Biospec Products, Bartlesville, OK) in the presence of two steel BB air gun beads (BB refers to the bead size, 4.5-mm diameter; Walmart Supercenter, Bentonville, AR, USA).

2.4 | Quantitative real-time PCR

qPCR was performed to determine presence/absence of HLB in healthy (HL), HLB early (asymptomatic) (HLB), HLB trees with blight (HLB-BL), and trees with symptoms of canker (CA leaf) DNA using 16S rDNA-based TaqMan primer-probe sets.[24] The qPCR assays were performed using an ABI 730 Real-Time PCR Detection System (Applied Biosystems/Thermofisher, USA) with the TaqMan Universal Master Mix II™ (Thermofisher, USA). qPCR was performed using the following conditions: one cycle at 95°C for 5 min, 40 two-step cycles each at 95°C for 15 s, and 60°C for 30 s. Approximately 100 ng of DNA was used as template per sample, and results were analyzed and recorded as Ct (threshold cycle) values. For this study, samples with a Ct value of ≤32 were considered as HLB positive (Figure S1).

2.5 | Multivariate data analysis.

SIMCA 14 (Umetrics, Umeå, Sweden) was used for statistical analysis of the collected Raman spectra. All imported spectra were scaled to unit variance to give all spectral regions equal importance. Orthogonal partial least squares discriminant analysis (OPLS-DA) was performed in order to determine the number of significant components and identify spectral regions that best explain the separation between the classes. In order to give each of the spectral regions equal importance, all spectra were scaled to unit variance. Raw spectra, containing wavenumbers 350–2,000 cm^{-1}, were retained in the model that resulted from this iteration of OPLS-DA.

3 | RESULTS AND DISCUSSION

We collected Raman spectra from leaves of HLB positive orange trees that had signs of blight (HLB + BL). We also collected spectra from trees that were HLB positive (HLB) by PCR and had no visual appearance of leaf yellowness (asymptomatic) and trees with canker (CA) that were PCR negative for HLB. Finally, we collected Raman spectra from in-field grown healthy orange trees (HL) that were confirmed to be HLB negative by PCR

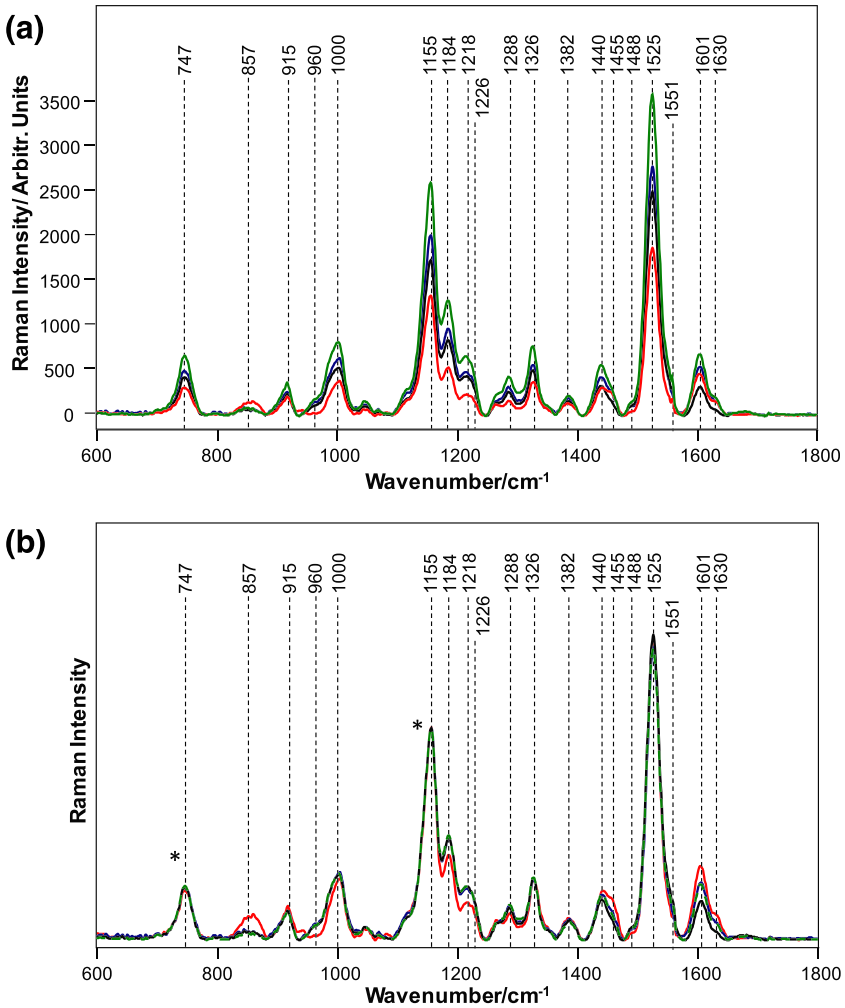

FIGURE 1 (a) Averaged raw and (b) normalized Raman spectra collected from leaves of healthy (dashed green), Huanglongbing (HLB) positive (red), canker (black), and HLB positive with blight (blue) orange trees. Spectra normalized on 1,382 cm^{-1} vibrational band, which were assigned to CH_2 vibration (marked by asterisk [*]) [Colour figure can be viewed at wileyonlinelibrary.com]

and had no visual symptoms characteristic for any known citrus disease.

We found that averaged Raman spectra collected from leaves of HLB, CA, and HLB + BL exhibited much lower intensities of all vibrational bands comparing with the spectra collected from leaves of HL plants (Figure 1 a). Interestingly, HLB plants showed the lowest spectral intensities from all four studied plant types. Such a change in the intensities of all vibrational bands can be associated with a decrease in the chlorophyll content of the leaf. However, the intensity profile alone cannot be utilized for confirmatory disease diagnostics. In our previous work, we proposed to normalize Raman spectra on 1,382 cm^{-1} vibrational band, which were assigned to CH_2 vibration (Table 1).[23] This chemical group is present in nearly all classes of biological molecules, which makes this normalization approach unbiased to the specific chemical component of the plant leaf. We showed that such unbiased normalization allowed for elucidation of the "spectroscopic fingerprint" that was unique for HLB and nutrient deficiency on both orange and grapefruit trees.[23] Following this normalization approach, we compared averaged spectra collected from HL, HLB, CA, and HLB + BL (Figure 1b).

We found that normalized Raman spectra collected from leaves of HLB positive orange trees exhibited an increase in intensities of 1,601–1,630 and 1,440–1,455 cm^{-1} vibrational bands, which could be assigned to lignin and aliphatic vibrations, respectively (Figure 1b). We also observed a decrease in the intensity of 1,184, 1,218, and 1,226 cm^{-1} bands in the spectra collected from leaves of HLB orange trees compared with HL, CA, and HLB + BL. We found that intensity of lignin bands in the spectrum of CA was lower compared with the averaged spectrum of HL plants. Surprisingly,

TABLE 1 Vibrational bands and their assignments for eaves of HL, HLB, CA, and HLB + BL collected from orange trees

Band	Vibrational mode	Assignment
747	γ(C—O—H) of COOH	Pectin[25]
915	ν(C—O—C) in plane, symmetric	Cellulose and lignin[26]
1,000	ν_3 (C—CH_3 stretching) and phenylalanine	Carotenoids and protein[27,28]
1,155	asym ν(C—C) ring breathing	Carbohydrates and cellulose[26]
1,184	ν(C—O—H) next to aromatic ring+σ (CH)	Xylan[29,30]
1,218–1,226	δ(C—C—H)	Aliphatic[31] and xylan[29]
1,247	C—O stretching (aromatic)	Lignin[32]
1,288	δ(C—C—H)	Aliphatic[31]
1,326	δCH_2 bending vibration	Cellulose and lignin[26]
1,382	δCH_2 bending vibration	Aliphatic[31]
1,440	δ (CH_2) + δ (CH_3)	Aliphatic[31]
1,455	δCH_2 bending vibration	Aliphatic[31]
1,488	δ (CH_2) + δ (CH_3)	Aliphatic[31]
1,527–1,551	—C=C— (in plane)	Carotenoids[33,34]
1,601	ν(C—C) aromatic ring+σ (CH)	Lignin[35,36]
1,630	C=C—C (ring)	Lignin[35–37]

TABLE 2 OPLS-DA confusion matrix of HLB + BL, CA, HL, and HLB spectra collected from leaves of orange trees

	Members	Correct	HLB + BL	CA	HL	HLB
HLB + BL	50	96.0%	48	2	0	0
CA	40	95.0%	1	38	1	0
HL	49	87.7%	6	0	43	0
HLB	47	89.4%	2	2	1	42
Total	186	92.0%	57	42	45	42

Abbreviations: OPLS-DA, orthogonal partial least squares discriminant analysis.

intensities of all other bands in the spectra collected from leaves of CA and HLB + BL exhibited only very small variations compared with the spectra collected from leaves of HL trees.

Next, we used OPLS-DA to achieve quantitative diagnostics of HLB, CA, and HLB + BL on orange trees. The loading plot and misclassification table were generated using the model that contained three predictive components, one orthogonal component, and 1,100 (601–1,700 cm^{-1}) original wavenumbers for standard normal variate preprocessed first derivative spectra (Figure S2). Predictive components (PCs) 1, 2, and 3 explained 22%, 21%, and 10% of variation between the different classes, respectively. Absolute intensities in the loadings spectra were proportional to the percentage of the total variation between classes explained by each wavenumber within each component.

The model identified the carotenoids peak at 1,525 cm^{-1} (PC1); lignin peaks at 1,601 and 1,630 cm^{-1} (PC1); cellulose peaks at 915 and 1,326 cm^{-1} (PC1); the xylan band at 1,184 cm^{-1} (PC2); the hydrocarbons bond vibration at 1,440, 1,455, and 1,488 cm^{-1} (PC2); and the cellulose and lignin peak at 1,630 cm^{-1} (PC3) as the strongest predictors of the pathogens, which supports the conclusions of our qualitative spectral analysis presented above. The model also explained 44% of the variation (R2X) in the spectra and 53% (R2Y) of the variation between the classes (Table 2).

In conclusion, we demonstrated that RS, coupled to advanced multivariate statistical analysis, can potentially be used for highly accurate diagnostics of blight on HLB-infected orange trees. Our results also indicate that RS could be used to distinguish between HLB and HLB + BL. Finally, we provided experimental evidence that RS can be used to distinct between HL, CA, HLB, and HLB + BL. Such a fast and reliable spectroscopic approach is highly important for successful intervention and management of HLB-infected trees. Specifically, our results indicated that CA and HLB + BL could be detected and identified with 95% and 96% accuracy, respectively. The accuracy of prediction of HL and HLB was 87.7 and 89.4%, respectively.

ACKNOWLEDGEMENTS

This study was supported by funds from T3 grant, Texas A&M University, Texas A&M AgriLife Research, Texas A&M University, Governor's University Research Initiative (GURI) grant program of (12-2016/M1700437) to D. K. and Texas A&M AgriLife Research Insect Vectored Diseases Seed Grant (124185-96210) to K. K. M.

CONFLICT OF INTEREST

None.

ORCID

Kranthi Mandadi https://orcid.org/0000-0003-2986-4016
Dmitry Kurouski https://orcid.org/0000-0002-6040-4213

REFERENCES

[1] J. M. Bové, *J. Plant Pathol.* **2006**, *88*, 7.

[2] J. K. Morgan, L. Zhou, W. Li, R. G. Shatters, M. Keremane, Y. P. Duan, *Mol. Cell. Probes* **2012**, *26*, 90.

[3] J. H. Tsai, Y. H. Liu, *J. Econ. Entomol.* **2000**, *93*, 1721.

[4] W. T. Swingle, J. H. Weber, *USDA Div. Veg. Physiol. Pathol. Bull. 1896*(8), 9.

[5] L. G. Albrigo, R. H. Young, *Horticult. Sci.* **1981**, *16*, 158.

[6] M. Cohen, R. R. Pelosi, R. H. Brlansky, *Phytopathology* **1983**, *73*, 1125.

[7] K. S. Derrick, L. W. Timmer, *Annu. Rev. Phytopathol.* **2000**, *38*, 181.

[8] R. F. Lee, L. J. Marais, L. W. Timmer, J. H. Graham, *Plant Dis.* **1984**, *68*, 511.

[9] H. K. Wutscher, M. Cohen, R. H. Young, *Plant Dis Rep* **1977**, *61*, 572.

[10] K. S. Derrick, R. F. Lee, R. H. Brlansky, L. W. Timmer, B. G. Hewitt, G. A. Barthe, *Plant Dis* **1990**, *74*, 168.

[11] L. Vauterin, B. Hoste, K. Kersters, J. Swings, *Int. J. Syst. Bacteriol.* **1995**, *45*, 472.

[12] E. L. Civerolo, F. Fan, *Plant Dis.* **1982**, *66*, 231.

[13] R. E. Stall, E. L. Civerolo, *Annu. Rev. Phytopathol.* **1991**, *29*, 399.

[14] M. Goto, in *Plant Diseases of International Importance*, (Eds: J. Kumar, H. S. Chaube, U. S. Singh, A. N. Mukhopadhyay), Prentice Hall, Englewood Cliffs, NJ **1992** 250.

[15] M. Goto, Y. Yaguchi, *Ann. Phytopathol. Soc. Japan* **1979**, *45*, 689.

[16] T. R. Gottwald, R. C. McGuire, S. Garran, *Phytopathology* **1988**, *78*, 739.

[17] J. Cubero, J. H. Graham, *Appl. Environ. Microbiol.* **2002**, *68*, 1257.

[18] M. Golmohammadi, J. Cubero, J. Penalver, J. M. Quesada, M. M. Lopez, P. Llop, *J. Appl. Microbiol.* **2007**, *103*, 2309.

[19] A. M. Alvarez, A. A. Benedict, C. Y. Mizumoto, L. W. Pollard, E. L. Civerolo, *Phytopathology* **1991**, *81*, 857.

[20] C. Farber, D. Kurouski, *Anal. Chem.* **2018**, *20*, 3009.

[21] V. Egging, J. Nguyen, D. Kurouski, *Anal. Chem.* **2018**, *90*, 8616.

[22] L. Sanchez, C. Farber, J. Lei, K. Zhu-Salzman, D. Kurouski, *Anal. Chem.* **2019**, *91*, 1733.

[23] L. Sanchez, S. Pant, Z. Xing, K. Mandadi, D. Kurouski, *Anal. Bioanal. Chem.* **2019**, *411*, 3125. https://doi.org/10.1007/s00216

[24] W. Li, J. S. Hartung, L. Levy, *J. Microbiol. Methods* **2006**, *66*, 104.

[25] A. Synytsya, J. Čopíková, P. Matějka, V. Machovič, *Carbohydr. Polym.* **2003**, *54*, 97.

[26] H. G. Edwards, D. W. Farwell, D. Webster, *Spectrochim. Acta A Mol. Biomol. Spectrosc.* **1997**, *53A*, 2383.

[27] N. Tschirner, K. Brose, M. Schenderlein, A. Zouni, E. Schlodder, M. A. Mroginski, P. Hildebrandt, C. Thomsen, *Phys Status Solidi (b)* **2009**, *246*, 2790.

[28] D. Kurouski, R. P. Van Duyne, I. K. Lednev, *Analyst* **2015**, *140*, 4967.

[29] U. P. Agarwal, *Front. Plant Sci.* **2014**, *5*, 1.

[30] Y. S. Mary, C. Y. Panicker, H. T. Varghese, *Orient J Chem* **2012**, *28*, 937.

[31] M. M. Yu, H. G. Schulze, R. Jetter, M. W. Blades, R. F. Turner, *Appl. Spectrosc.* **2007**, *61*, 32.

[32] Y. Cao, D. Shen, Y. Lu, J. Huang, *Ann. Bot.* **2006**, *97*, 1091.

[33] G. Devitt, K. Howard, A. Mudher, S. Mahajan, *ACS Chem. Nerosci.* **2018**, *9*, 404.

[34] F. Adar, *Spectroscopy* **2017**, *32*, 12.

[35] L. Kang, K. Wang, X. Li, B. Zou, *J. Phys. Chem. C* **2016**, *120*, 14758.

[36] U. P. Agarwal, *Planta* **2006**, *224*, 1141.

[37] D. R. Pompeu, Y. Larondelle, H. Rogez, O. Abbas, J. A. F. Pierna, V. Baeten, *Biotechnol. Agron. Soc. Environ.* **2017**, *22*, 1.

SUPPORTING INFORMATION

Additional supporting information may be found online in the Supporting Information section at the end of the article.

How to cite this article: Sanchez L, Pant S, Irey M, Mandadi K, Kurouski D. Detection and identification of canker and blight on orange trees using a hand-held Raman spectrometer. *J Raman Spectrosc*. 2019;1–6. https://doi.org/10.1002/jrs.5741